Journal Pre-proof

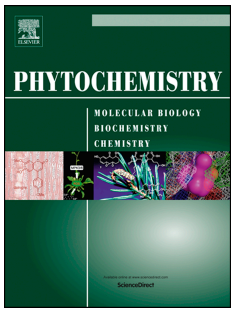

Metabolic adaptation of diatoms to hypersalinity

Vera Nikitashina, Daniel Stettin, Georg Pohnert

PII: S0031-9422(22)00183-2

DOI: https://doi.org/10.1016/j.phytochem.2022.113267

Reference: PHYTO 113267

To appear in: *Phytochemistry*

Received Date: 4 April 2022

Revised Date: 20 May 2022

Accepted Date: 29 May 2022

Please cite this article as: Nikitashina, V., Stettin, D., Pohnert, G., Metabolic adaptation of diatoms to hypersalinity, *Phytochemistry* (2022), doi: https://doi.org/10.1016/j.phytochem.2022.113267.

Exposure of algae to salinity stress

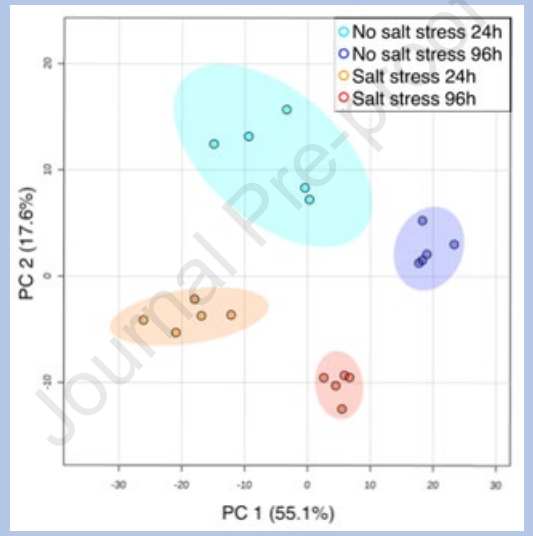

Monitoring of the metabolic response

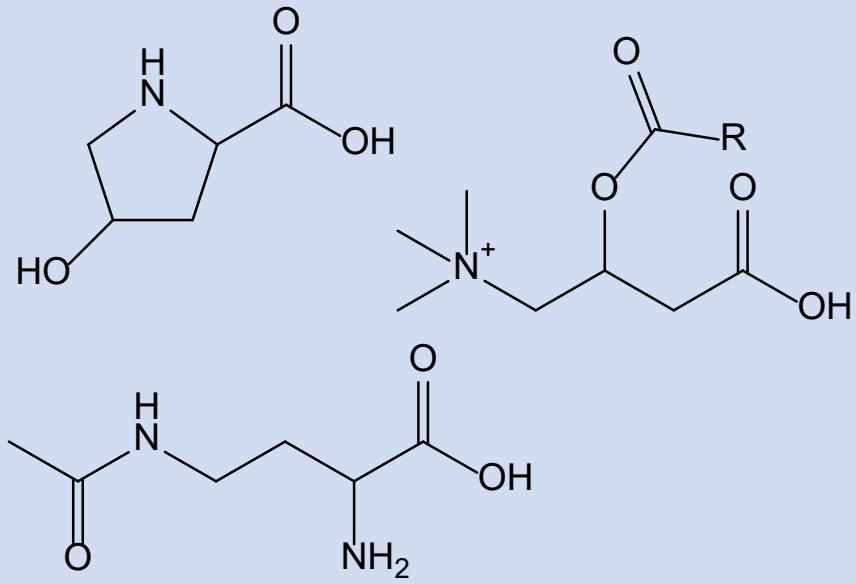

Identification of dysregulated metabolites and pathways

Metabolic adaptation of diatoms to hypersalinity

Vera Nikitashina[1,a], Daniel Stettin[1,a], Georg Pohnert[a]*,

*E-mail georg.pohnert@uni-jena.de, tel. +49 3641 948170

[a]Institute for Inorganic and Analytical Chemistry, Bioorganic Analytics, Friedrich Schiller University Jena, 07743 Jena, Germany

[1] Authors contributed equally to this paper

Abstract

Microalgae are important primary producers and form the basis for the marine food web. As global climate changes, so do salinity levels that algae are exposed to. A metabolic response of algal cells partly alleviates the resulting osmotic stress. Some metabolites involved in the response are well studied, but the full metabolic implications of adaptation remain unclear. Improved analytical methodology provides an opportunity for additional insight. We can now follow responses to stress in major parts of the metabolome and derive comprehensive charts of the resulting metabolic re-wiring. In this study, we subjected three species of diatoms to high salinity conditions and compared their metabolome to controls in an untargeted manner. The three well-investigated species with sequenced genomes *Phaeodactylum tricornutum*, *Thalassiosira pseudonana*, and *Skeletonema marinoi* were selected for our survey. The microalgae react to salinity stress with common adaptations in the metabolome by amino acid up-regulation, production of saccharides, and inositols. But also species-specific dysregulation of metabolites is common. Several metabolites previously not connected with osmotic stress reactions are identified, including 4-hydroxyproline, pipecolinic acid, myo-inositol, threonic acid, and acylcarnitines. This expands our knowledge about osmoadaptation and calls for further functional characterization of metabolites and pathways in algal stress physiology.

Keywords

Phaeodactylum tricornutum; Phaeodactylaceae; *Thalassiosira pseudonana*; Thalassiosiraceae; *Skeletonema marinoi*; Skeletonemataceae; Diatomic algae; Hypersalinity stress response; Osmolytes; Untargeted metabolite profiling.

1. Introduction

Phytoplankton is estimated to be responsible for roughly 50% of global primary production and forms the basis of the marine food web (Field et al., 1998). Algal cells

forming the phytoplankton experience environmental fluctuations in their habitat during sinking or transport by currents. Shifts in nutrient availability, light and temperature (Vidal et al., 2017) can lead to a change in the species composition of the phytoplanktonic community. However, these factors also influence the physiology of the persisting cells. On the long term, global warming alters the productivity and composition of phytoplankton (Thomas et al., 2012). Additional parameters connected to temperature, like dissolved CO_2 and salinity, influence the algae as well (Sugie et al., 2020). Surface salinity patterns, mainly influenced by increasing evaporation and precipitation or other freshwater influx, are becoming more important on a global level due to climate change (Durack and Wijffels, 2010; Zika et al., 2018). Because algae are surface-dwelling primary producers, they are directly affected by such changes in ocean salinity. Considering the importance of phytoplankton for global primary production, it is vital that we understand the effect of alterations in salinity concerning growth, community composition and metabolism.

A change in salinity in the aqueous environment of a phytoplankton cell subjects it to osmotic stress. This can be alleviated by water flux in or out of the cell or adjustment of the intracellular salt concentration. These salts include inorganic ions and organic compatible solutes, called osmolytes (Kirst, 1989). The accumulation of osmolytes is believed to be the most widespread and long-term successful mechanism of osmoadaptation to increased salinity in free-living algae (Ochsenkühn, 2017).

The main body of literature about the identity and quantity of organic osmolytes in microalgae stems from targeted analytics (Hellebust, 1976; Dickson, 1987). Modern untargeted screening using high-resolution mass spectrometry can offer additional insight (Thume et al., 2018) and reveal previously unrecognized metabolic connections. The opportunity to unravel novel aspects in algal physiology prompted us to perform a salt-stress experiment on diatoms and analyze extracts with liquid- and gas-chromatography coupled to high-resolution mass spectrometry in an untargeted manner. This revealed metabolites and pathways responding to salinity changes and allowed us to document metabolic networks connected to osmoadaptation.

For this study, we choose three diatom species – *Phaeodactylum tricornutum* Bohlin (Phaeodactylaceae), *Thalassiosira pseudonana* Hasle & Heimdal (Thalassiosiraceae) and *Skeletonema marinoi* Sarno & Zingone (Skeletonemataceae) – as model organisms. These algae are well-investigated with sequenced genomes and a wealth of knowledge on their physiology (Armbrust et al., 2004; Bowler et al., 2008; Johansson et al., 2019). Since different microalgal species may react to hypersalinity with individual changes

in their metabolic profile, we aimed to compare the three diatom responses to unravel joint and unique physiological adaptations (Dickson, 1987; Gebser and Pohnert, 2013; Scholz and Liebezeit, 2012). We observed dysregulation of 5% to 46% from all detected compounds. We connect multiple new compounds including 4-hydroxyproline, pipecolinic acid, myo-inositol, threonic acid, acylcarnitines to osmoadaptation in microalgae.

2. Results

To best mimic natural non-limiting conditions and at the same time obtain a high number of cells for extraction, salinity stress experiments were performed with algal cultures in the later logarithmic growth phase. Relatively high salt concentration for the stress (initially 60 PSU) was selected so that it could induce significant changes in the algal endometabolome. We adjusted salinity stress so that it does not lead to algal cell death since otherwise changes in the endometabolome would be associated with cell death processes. The elevation of medium salinity to values close to 60 PSU was previously performed to investigate the effect of increased salinity on the growth, and metabolome of diatoms (Bergeijk et al., 2003; Rijstenbil, 2003; García et al., 2012; Jaramillo-Madrid et al., 2020).

In this study, analysis of the stress response was performed at two time points after salinity increase. A short-term salinity stress response was analyzed 24 hours after the stress, which is on average less than doubling time of diatoms (Laws, 2013). Thus, direct response of the cells was analyzed. The long-term response was examined 96 hours after the increase in salt content when algal cells could divide at least two times. Consequently, salinity stress adaptation of the next generations could be examined.

2.1. Effect of the salinity stress on the growth rate of diatoms

To analyze the effect of increased salinity on the growth of the algae, chlorophyll fluorescence intensity and cell density of the cultures were monitored.

P. tricornutum and *T. pseudonana* tolerated the salinity stress at 60 PSU and exhibited growth during at least four days after the stress (Fig. S1, S2). However, lower cell numbers and chlorophyll fluorescence intensity compared to the control were observed (statistically significant p-value <0.05) for both time points for both diatoms.

Elevation of salinity of *S. marinoi* cultures led to the dramatic decrease almost to zero in both chlorophyll fluorescence intensity and cell density 96 hours after 60 PSU treatment, while the control cultures showed normal growth. Furthermore, this diatom

showed no growth under 55 PSU salinity stress (Fig. S3). At 50 PSU *S. marinoi* cultures showed almost no decrease in both chlorophyll fluorescence intensity and cell density 24 hours after the treatment and grew at least four days at elevated salinity (Fig. S4). The reduction of chlorophyll and cell counts after salinity stress treatment was statistically significant compared to control cultures for both time points.

Therefore, for diatoms *P. tricornutum* and *T. pseudonana* analysis of endometabolome changes in response to salinity increase was performed at 60 PSU and endometabolic changes of *S. marinoi* were analyzed in response to the salinity increase to 50 PSU.

2.2. Changes in the endometabolome composition of *T. pseudonana* in response to short term salinity stress

Salinity stress led to significant changes in the *T. pseudonana* endometabolome as indicated by a clear separation in PCA plots of stressed and control cultures after 24 h (Fig. 1).

A volcano plot analysis was conducted to assess significantly dysregulated metabolites (Fig. S5, S6). Compounds were considered to be significantly dysregulated in response to the salinity stress when their fold change in comparison to the controls was more than 2 or less than 0.5, with a *p*-value less than 0.05. In response to the short-term salinity stress, volcanoe plots revealed a statistically significant dysregulation of 102 compounds for the GC-MS results for *T. pseudonana*, which was around a quarter of all detected compounds. Only three dysregulated compounds were down-regulated; all others increased in concentration (cell count normalized data).

Among the identified metabolites detected with GC-MS, pipecolinic acid and proline exhibited the highest increase in concentration. In total, up-regulation of 11 amino acids was observed. Also, increase in content of 8 sugars (one disaccharide, five monosaccharides, and two inositols) was detected (Table S1).

Statistical analysis of the LC-MS results of *T. pseudonana* short-term salinity stress response revealed significant increase in concentrations for 50 compounds. That was almost half of all detected compounds, and only of one compound the concentration decreased significantly in comparison to the controls. The most up-regulated among the identified metabolites were arginine, the ectoine precursor *N*γ-acetyldiaminobutyrate, and ectoine (Table S1).

2.3. Changes in the endometabolome composition of *T. pseudonana* in response to the long-term salinity stress

In response to the long-term salinity stress, statistically significant dysregulation was shown for 85 compounds detected with GC-MS. Six of them were down-regulated, and

the content of 79 was increased (cell count normalized data) (Fig. S7). Among identified metabolites, only citric acid showed a decrease in content, while contents of others were increased. Similar to the short-term salinity stress response, the most up-regulated identified compounds were amino acids and amines, including proline and pipecolinic acid. Their fold changes increased compared to the values at the 24 hours time point. Also increase of pyrrole-2-carboxylic acid and threonine was observed (Table S1).

Statistical analysis of the LC-MS results for the long-term salinity stress response revealed dysregulation of 39 compounds (Fig. S8). This complementary analytical method confirmed the increase in proline and pipecolinic acid. Also, up-reguation of ectoine and its precursor was detected.

2.4. Comparison of short- and long-term salinity stress responses of *T. pseudonana*

The number of significantly dysregulated metabolites detected with both analytical methods decreased over the diatom's salinity stress adaptation period. In GC-MS data, 56 up-regulated compounds at both time points were detected. For 29 of them, an increase in fold change during the adaptation was shown. LC-MS results revealed 34 commonly up-regulated metabolites, and the fold changes for 26 of them increased in the sample extracted after 96 hours in comparison to the 24 hours time point. Thus, for the majority of the common compounds an increase in fold change was detected with both methods 96 hours after the stress. Consequently, it can be hypothesized that the reduction in number of up-regulated compounds over time is due to them being replaced by higher concentrations of compatible solutes that serve to support cells in long-term stress situations. Examples of such compounds would be proline and two betaines – glycine betaine and proline betaine, which were not among significantly dysregulated compounds 24 hours after the stress but up-regulated after 96 h.

The four treatments formed separate groups when control and stress GC-MS samples from two time points were compared in a PCA. In data from LC-MS analysis, there is an overlap in principal components 1 and 2 (samples 24 hours control and 96 hours high salinity) that was resolved by plotting three principal components (Fig. 1, Fig. S9).

2.5. Changes in the endometabolome composition of *P. tricornutum* in response to the short- and long-term salinity stresses

For *P. tricornutum*, salinity stress also triggered significant changes in endometabolome composition. Separation between stressed and control cultures was observed in the PCA analysis of GC-MS and LC-MS data for both time points (Fig. 2).

In response to the short-term salinity stress, the statistical analysis revealed an increase in content for the majority of the dysregulated compounds normalized to cell count. Only for one out of 69 dysregulated compounds detected with GC-MS down-regulation was shown, all 89 statistically significant compounds detected with LC-MS were up-regulated (Fig. S10, S11).

Among metabolites detected with GC-MS, the highest increase was observed for a putatively identified glyceryl-glycoside in response to short- and long-term salinity stresses. Interestingly, up-regulation of the same metabolite was also detected for *T. pseudonana* at both time points but with comparatively lower fold changes.

As for *T. pseudonana*, mainly amino acids and saccharides were among the identified up-regulated compounds. Also, similarly to *T. pseudonana*, up-regulation of pyrrole-2-carboxylic and threonic acid, ectoine, and its precursor *N*γ-acetyldiaminobutyrate was detected for this alga (Table 1).

In contrast to *T. pseudonana*, increased concentrations of methyl palmitate, putrescine, and butyrylcarnitine were detected for *P. tricornutum* in response to the short-term salinity stress. Interestingly, in response to the long-term salinity stress butyrylcarnitine was not present among significantly up-regulated compounds, but increase in content of another acylcarnitine – propionylcarnitine was detected. Furthermore, statistically significant increase in the content of cysteinolic and pipecolinic acids, methionine, and adenosine was detected 96 hours but not 24 hours after the salinity stress for *P. tricornutum* (Table S2).

No clear pattern was found for the long term adaptation. The amount of significantly dysregulated compounds detected with GC-MS decreased from 69 to 49 during the 96 hours salinity stress adaptation of the algae (Fig. S12). For the LC-MS analysis, the number of statistically significantly changed metabolites conversely rose from 89 to 113 in course of time (Fig. S13).

PCA also showed two different trends for GC- and LC-MS analysis. According to the GC-MS results, the endometabolome composition of *P. tricornutum* was affected to a larger extent by the cultivation time than by salinity elevation (Fig. 2E). Cultures extracted at different time points were located further from each other than control and treated cultures from the same time point. Whereas, for LC-MS the clustering of treated and control cultures can be observed. High variation among stressed cultures at 24 hours led to overlap with both control at 24 hours and stressed cultures at 96 hours (Fig. 2F).

2.6. Changes in the endometabolome composition of *S. marinoi* in response to the short- and long-term salinity stresses

Both *P. tricornutum* and *T. pseudonana* were subjected to salinity stress of 60 PSU. However, *S. marinoi* showed no further growth at salinities of 60 or 55 PSU. For this reason, the analysis of the endometabolome composition for this diatom was investigated in response to the increase in salt concentration to 50 PSU where it still grew.

Similar to the results obtained for two other diatoms, salinity stress led to significant changes in the endometabolome composition (Fig. 3). Consitently with the data from the other diatoms, increase in cell count normalized metabolite concentrations was also observed for *S. marinoi* as a response to the salinity stress.

An increase in amino acid content, especially in proline and 4-hydroxyproline, was detected in salinity stressed cultures of *S. marinoi* (Table S3). Interestingly, conversely to results obtained for *P. tricornutum* and *T. pseudonana*, no saccharide accumulation was detected for *S. marinoi* in response to the elevation of the salt content at any time point. However, the up-regulation of both myo- and scyllo-inositols and putatively identified glyceryl-glycoside was observed for *S. marinoi* in response to the long-term salinity stress. Also, similar to the two other diatoms, the concentration of pyrrole-2-carboxylic acid was increased in stressed cultures of *S. marinoi* at both analyzed time points.

Furthermore, an increase in the content of four different acylcarnitines was observed for this diatom in response to the short-term salinity stress. Butyrylcarnitine and propionylcarnitine were also detected in *P. tricornutum*, two others unique to *S. marinoi* were acetylcarnitine and isovalerylcarnitine. Moreover, similar to *P. tricornutum*, content of cysteinolic acid increased in salinity stressed cultures at both analyzed time points (Table 1).

Similar to *T. pseudonana*, an increase in glycine betaine content was observed in high-salinity cultures of *S. marinoi*. Statistically significant up-regulation of glycine betaine was detected at both time points for this diatom.

Overall, the number of significantly dysregulated compounds detected with GC-MS increased from 21 to 51 over time of salinity stress adaptation (Fig. S14, S16). Almost all significantly increased metabolites after 24 hours were also significantly up-regulated 96 hours after the treatment (19 out of 21). Conversely, the number of metabolites detected with LC-MS 24 hours after the stress was higher than at 96 hours time point (62 compounds detected for the 24 hours time point, compared to 22 detected

for the 96 hours time point) (Fig. S15, S17). In turn, 18 out of 22 up-regulated metabolites after 96 hours were the same as at 24 hours. Down-regulation was detected only with LC-MS for three compounds 96 hours after the treatment. Two of these metabolites (one of them leucine) were elevated 24 hours after the stress exhibiting a transient maximum.

2.7. Comparison of salinity stress responses of *P. tricornutum, T. pseudonana,* and *S. marinoi*

We compared the amount of unique and shared metabolites regulated in response to salinity stress between the three diatoms. Surprisingly, only ca. 6 % after 24 h and 4% after 96 h of the metabolites were common for a salinity adaptation in all three investigated species. This corresponds to 22 common metabolites (8 detected in GC-MS, 13 in LC-MS, and proline detected with both methods) that were significantly dysregulated in all species at least at one time point. All of them were up-regulated.

A pairwise analysis shows that *P. tricornutum* and *T. pseudonana* share more commonly dysregulated metabolites compared to S. *marinoi* and *T. pseudonana* or *S. marinoi* and *P. tricornutum* (Fig. 4 and 5). The largest share of dysregulated metabolites was unique for individual algal species and the vast majority of all dysregulated metabolites were up-regulated upon salinity increase.

3. Discussion

3.1. Influence of the salinity stress on the growth of diatoms

Salinity is almost constant in the open oceans and varies only little between 33 and 37 PSU. In nearshore waters, however, salinity fluctuations are substantial. Future climate change scenarios predict increased changes in water salinity due to evaporation or reduced freshwater intake from rivers due to low precipitation (Glaser and Karsten, 2020).

Diatoms can tolerate much higher salinity changes than the salinity ranges of their original habitat (Yamamoto et al., 2017). It was, however, observed that an increase in salinity negatively correlates with growth rates and affects the chemical composition of diatoms (Bergeijk et al., 2003; Rijstenbil 2003; García et al., 2012; Jaramillo-Madrid et al., 2020). We opted to evaluate the physiological and metabolic response of three model diatoms to extreme salinity stress. We initially tested their tolerance to hypersalinity to avoid stress resulting in culture death. After salinity increase to 60 PSU *P. tricornutum* and *T. pseudonana* responded with a strongly reduced growth compared to the control. Both algae continued to divide and the chlorophyll content of the culture increased under control and salinity stress conditions (Fig. S1-S2). This confirms

277 previous findings of salt tolerance for these two algae (Jaramillo-Madrid et al., 2020).
278 *S. marinoi* was not as tolerant towards increased salinity regimes and did not grow at a
279 salinity over 50 PSU (Fig. S3-S4). This is in accordance with a survey of Branda, who
280 determined growth of this alga at 5 to 45 PSU (Branda, 1984).
281 Kirst suggested that growth rate is affected due to the inhibitory effect of high ion
282 concentration on the metabolic processes. Moreover, the synthesis of organic osmolytes
283 could take resources from general metabolism (Kirst, 1989). The negative effect of the
284 salinity stress on the photosystems could be caused by increased permeability of the
285 thylakoid membrane to ions, including Na^+ and CI^-, inhibiting both photosystems. This
286 effect was previously shown in the unicellular green alga *Dunaliella tertiolecta*
287 (Gilmour et al., 1982; Gilmour et al., 1985).

288 **3.2. Significantly dysregulated metabolites and their possible interconnections**

289 The most widespread adaptation mechanism of diatoms to osmotic changes in their
290 environment is the adjustment of the cellular concentration of compatible solutes
291 (Ochsenkühn et al., 2017). Many studies address the regulation of such metabolites
292 mainly based on the targeted analysis of candidate compounds. Amino acids and their
293 metabolites are common up-regulated compounds upon hypersalinity stress. Also,
294 organic sulfur compounds, including the dominant dimethylsulfoniopropionate
295 (DMSP), have been quantitatively surveyed (Dickson and Kirst, 1987; Gebser and
296 Pohnert, 2013). We set out here to determine the metabolome changes of three model
297 diatoms with an untargeted approach. This allows the identification of common and
298 unique compatible solutes in the diatoms and linking the dysregulated metabolites to
299 metabolic pathways. We used an analytical approach based on high-resolution mass
300 spectrometry. By combining GC-MS and LC-MS analysis, we could reach an
301 unprecedentedly broad metabolic coverage of up to 344 features with GC-MS and 548
302 features with LC-MS.
303 The survey of three diatom species introduced in this study indicates that all of them
304 respond predominantly with increasing concentrations of intracellular metabolites to
305 hypersalinity stress. Only a few compounds were found in lower concentrations, which
306 is in accordance with the concept of increasing intracellular osmolyte production upon
307 hypersalinity stress. We identified surprisingly few metabolites that are up-regulated in
308 all three investigated species. These include amino acids, amines and a myo-inositol.
309 Most of these metabolites were previously identified in targeted analyses of diatom
310 responses (Dickson and Kirst, 1987; Scholz and Liebezeit, 2012; Gebser and Pohnert,
311 2013). The majority of identified metabolites were, however, unique to the respective

species, which indicates a surprising individuality within diatoms. This uniqueness is not caused by their phylogenetic position, with *T. pseudonana* and *S. marinoi* belonging to the order Thalassiosirales and the Raphid Bacillariophyceae *P. tricornutum* to the Baccilariales (Medlin and Kaczmarska, 2004). Despite this relation, no increased metabolic overlap was detected in *T. pseudonana* and *S. marinoi* (Fig. 4 and 5).

3.2.1. Amino acids and their derivatives

Amino acids play an important role as compatible solutes. Accordingly, they comprise the most significant group among the identified dysregulated compounds in response to hyperosmotic stress (Table 1). Their accumulation was explained with continuing *de novo* amino acid biosynthesis and due to reduced protein synthesis (Hellebust, 1976; García et al., 2012). Alternatively, the high content of amino acids in response to osmotic stress could be caused by protein degradation, as shown for higher plants (Fukutoku and Yamada, 1981; Joshi et al., 2010).

In many organisms, proline is one of the main osmolytes accumulated in response to hyperosmotic stress (Adams et al., 1992). Over time, the increase in proline content was also detected for all three diatoms in this study under increased salinity. Similar responses were previously shown for diatoms, such as the small euryhaline *Cyclotella meneghiniana* and *C. cryptica*. These algae accumulate proline in response to the osmotic shock via biosynthesis using arginine and glutamate as substrates (Liu and Hellebust, 1976). In our study, arginine was also up-regulated by *T. pseudonana* at both time points.

Accumulation of 4-hydroxyproline and pyrrole-2-carboxylic acid was detected for all studied diatoms. These two metabolites are biosynthetically derived from proline. Accumulation of 4-hydroxyproline in response to salinity stress and its osmolytic function was reported in bacteria (Mimura et al., 1994; Kim et al., 2017). Increase in pyrrole-2-carboxylic acid upon salt and drought stress has also been found in higher plants (Kissoudis et al., 2015; Zhang et al., 2017). The role as an osmoprotectant in other species points towards a similar role in diatoms.

An increase in lysine content was detected for *P. tricornutum* and *T. pseudonana.* This amino acid is accumulated during water stress in plants (Fukutoku and Yamada, 1981). In the bacterium *Silicibacter pomeroyi*, lysine helps to cope with osmotic stress. Moreover, lysine might serve as a precursor to produce pipecolinic acid. This transformation is common for bacteria and plants, where pipecolinic acid plays a role as osmoprotectant (Moulin et al., 2000; Neshich et al., 2013). Based on the results

obtained in this work, the osmoprotectant role of pipecolinic acid is also plausible for diatoms, because its accumulation was detected for all three species.

Ectoine is a heterocyclic amino acid, which acts as compatible solute in halophilic and halotolerant prokaryotes. It is also found in some halophilic protists and microalgae (Peters et al., 1990; Czech et al., 2018; Weinisch et al., 2018; Fenizia et al., 2020). Ectoine is synthesized from aspartate with intermediate production of *N*γ-acetyldiaminobutyrate (Peters et al., 1990). Elevated levels of ectoine in response to salinity stress were detected for all studied diatoms at both time points analyzed. Accumulation of ectoine was previously described for diatoms, and an increase in its content in response to salinity stress was shown for *P. tricornutum* (Landa et al., 2017; Fenizia et al., 2020). Analysis of biosynthetic pathways, enabled by our metabolomics approach, can link the observed elevated levels of *N*γ-acetyldiaminobutyrate in *T. pseudonana* and *P. tricornutum* under salt stress to the up-regulation of ectoine biosynthesis.

For *S. marinoi*, dysregulation of leucine was detected. Notably, the amino acid was up-regulated in response to the short-term salinity stress and down-regulated in response to the long-term salinity stress. Possibly, this amino acid initially accumulated due to the general reduction of the protein synthesis or protein degradation. Later, it might be consumed in catabolism, providing an alternative source of acetyl-CoA to maintain the general metabolism (Mentzen et al., 2008).

3.2.2. Saccharides and polyols

Saccharides and polyols can serve as osmolytes themselves or be used for amino acid biosynthesis. The accumulation of saccharides in response to salinity stress was detected for *T. pseudonana* and *P. tricornutum*. Among identified saccharides, glucose, mannose, and cellobiose were common for these two algae. Accumulation of glucose and mannose was previously detected in the diatom *Nitzschia constricta* when the alga was exposed to a salinity of 50 PSU (Scholz and Liebezeit, 2012). In turn, mannose could be a substrate for threonic acid biosynthesis (Kanehisa and Goto, 2000). Previously, accumulation of threonate was shown in response to salinity stress in soybean (Zhang et al., 2016). An increase in the content of threonic acid was also detected for *T. pseudonana* and *P. tricornutum.* Interestingly, the fold change of mannose was higher than for threonic acid. Mannose is not only required for the synthesis of threonate but might play a role as an osmolyte by itself.

In addition to structural and signaling functions, inositols are also known as osmolytes (Downing et al., 2018). During myo-inositol biosynthesis, glucose-6-phosphate is

converted to myo-inositol, which protects cells from salinity-induced damage. For instance, kiwifruit accumulate myo-inositol in the first 24 hours after salinity stress (Klages et al., 1999). In the current study, up-regulation of myo-inositol was detected for *P. tricornutum* and *T. pseudonana* at 24 hours, and *S. marinoi* at 96 hours. Myo-inositol can be converted to scyllo-inositol (Kanehisa and Goto, 2000). This metabolite is suggested as an osmolyte in, for example, invertebrates of the deep-sea (Yancey, 2005; Downing et al., 2018). Up-regulation of both inositols was detected for *T. pseudonana* and *S. marinoi.*

In conclusion, this work confirms that saccharides are modulated in adaptation to the salinity stress for *P. tricornutum* and *T. pseudonana.* For *S. marinoi* no significant dysregulation of any saccharide was detected.

3.2.3. Quaternary ammonium and tertiary sulfonium derivatives

Quaternary ammonium compounds are another major class of osmolytes (Yancey, 2005). For the algae investigated, quaternary ammonium compounds, such as glycine betaine, proline betaine (stachydrine), and acylcarnitines could be identified among the significantly increased metabolites upon salinity stress.

Up-regulation of several acylcarnitines was detected for *P. tricornutum* and *S. marinoi* in response to hypersalinity. For *P. tricornutum*, an increase in the content of two acylcarnitines was detected after 24 and 96 hours. In *S. marinoi,* four acylcarnitines were in the list of up-regulated compounds 24 hours after salinity stress. A study on *Lactobacillus plantarum* showed that acylcarnitines could play a role as osmoprotectants, although not as effectively as carnitine itself. In contrast to our work, the carnitine derivative up-regulation went ahead with a reduction in accumulated amino acids in the bacteria (Kets and Bont, 1997). If the observed changes in acylcarnitines are connected to osmoadaptation or if they can be considered as a secondary response to altered amino acid biosynthesis has to be clarified in future studies.

Glycine betaine is a compatible solute found in pro- and eukaryotes (Yancey, 2005). Its accumulation in response to the salinity stress was described for several diatom species, including *P. tricornutum* and *T. pseudonana* (Keller et al., 1999; Martino et al., 2007; Scholz and Liebezeit 2012). During this work, up-regulation of glycine betaine was detected in *S. marinoi* at both time points and in *T. pseudonana* at 96 hours. Accumulation of proline betaine was detected for *T. pseudonana* in response to the long-term salinity stress. Its accumulation in response to salinity stress was reported for

several plants and algae, including the diatom *Nitzschia lecointei* (Blunden et al., 1992; Trinchant et al., 2004; Downing et al., 2018; Dawson et al., 2020).

Interestingly, dimethylsulfoniopropionate, a metabolite often discussed as diatom compatible solute was not among those compounds that were up-regulated according to our criteria. The metabolite was detected in all investigated diatoms but significant up-regulation could not be confirmed. This is in accordance with observations that more subtle osmoadaptations go ahead with the regulation of amino acids and quartery ammounium metabolites, while DMSP, that is highly abundant, only compensates salinity changes under extreme stress conditions (Gebser and Pohnert, 2013).

4. Conclusions

This work addresses the orchestrated metabolic response of diatom metabolism in response to hypersalinity. We can distinguish between universally up-regulated metabolites in all three diatoms under hypersalinity stress that support a common adaptation mechanism. Amino acids, saccharides and inositols were most conserved (Liu and Hellebust, 1976; Scholz and Liebezeit, 2012). The majority of regulated metabolites was specific to one or two species. The common repertoire of regulated metabolites is thus accompanied by species-specific physiological responses.

The untargeted screening introduced here allowed not only the detection of previously identified candidates. It led to the identification of several metabolites that were previously not associated with salinity stress response in diatoms, e.g. 4-hydroxyproline, pipecolinic acid, myo-inositol, threonic acid, and acylcarnitines. For some of these metabolites their osmoprotectant role was described in plants or bacteria (Mimura et al., 1994; Kets and Bont, 1997; Moulin et al., 2000; Neshich et al., 2013; Kim et al., 2017). Up-regulation of these metabolites was detected in at least for two of three studied diatoms.

We could also show that certain metabolites were specific for only short term or long term adaptation to hypersalinity. The data set introduced here, which is publicly accessible in the MetaboLights database, thus allows identifying common and specific processes in response to hypersalinity in diatoms. It will serve as a basis for future analysis of metabolic re-wiring of these unicellular algae under stress.

5. Experimental

5.1. Solvents

For endometabolome extraction, LC-, GC-MS sample, and analytical standard preparation (if not stated otherwise), the following reagents were used: methanol

(SupraSolv, Merck, Germany), ethanol (LiChrosolv, Supelco, Merck, Germany), chloroform (HPLC grade, Fisher Scientific, UK), acetonitrile (CHEMSOLUTE, Th. Geyer, Germany), water (Chromasolv Plus for HPLC, Honeywell, Germany).

5.2. Strains and culture conditions

Strains of *Phaeodactylum tricornutum* Bohlin (Phaeodactylaceae) CCMP 2561 and *Thalassiosira pseudonana* Hasle & Heimdal (Thalassiosiraceae) CCMP 1335 were obtained from the Bigelow National Center for Marine Algae and Microbiota (East Boothbay, USA), *Skeletonema marinoi* Sarno & Zingone (Skeletonemataceae) RCC 75 was obtained from the Roscoff Culture Collection (Roscoff, France). All cultures are maintained in the algae culture collection of the laboratory.

Cultures were grown in 50 mL cell culture flasks containing 40 mL of artificial seawater medium (ASW) (Maier and Calenberg, 1994). Stock cultures at the stationary phase were used for inoculation. Starting cell densities were $0.025 \cdot 10^6$ cells mL^{-1} for *P. tricornutum* and *T. pseudonan*, and $0.085 \cdot 10^6$ cells mL^{-1} for *S. marinoi*. The standard temperature was 13 °C and the light adjusted to 55-65 µmol photons m^{-2} s^{-1} with 14/10 light/dark cycle; all cultures were incubated with shaking at 80 rpm.

5.3. Experimental design

Pre-cultures of the algae were grown in triplicates until they reached stationary phase. Five culture replicates were inoculated for each treatment for the salinity stress experiments. ASW media blanks of the same volume were prepared in duplicates for each treatment. Salinity stress was initiated when cultures were at the late log-phase and the endometabolome was extracted 24 and 96 hours afterwards.

For *P. tricornutum* and *T. pseudonana,* salinity stress was performed by increasing the salt content in the medium from 35 to 60 PSU as described below.

To establish the upper salt concentration in the medium at which *S. marinoi* could grow, experiments with three different salt concentrations of 50, 55, and 60 PSU, were performed. Because negative growth was observed for salt concentrations above 50 PSU, the endometabolome analysis was performed for cultures subjected to the salt increase in the medium to 50 PSU.

5.4. Growth curves

For growth curve determination, cell amounts and growth rates were monitored by cell counting and chlorophyll fluorescence intensity. Samples were taken once every two to

three days during the cultivation period and right before, as well as one, two, and four days after the salinity stress.

Cell counting was conducted using a Fuchs Rosenthal Counting Chamber (Glaswarenfabrik Karl Hecht, Germany) under the light microscope Leica DM 2000 (Leica Microsystems, Wetzlar, Germany).

Chlorophyll fluorescence intensity measurement was conducted with a Varioskan Flash spectral scanning multimode reader (Thermo Scientific, Schwerte, Germany). The excitation wavelength was 430 nm, and the emission wavelength was 665 nm. Measurements were performed in the 96 well-plate format with 200 µL of well-mixed culture per well, each culture was measured in triplicates.

The final cell amount was normalized taking into account the extra medium added during the experiment. Statistical analysis was performed using two-sample t-test.

5.5. Salinity stress experiment

To perform the salinity stress experiments, 5 mL of 35 PSU ASW enriched with either 0.135 g mL^{-1}, 0.180 g mL^{-1}, or 0.225 g mL^{-1} of NaCl (Carl Roth, Germany) were added to 40 mL of cultures and media blanks (35 PSU) to reach the final salt concentrations of 50, 55, and 60 PSU respectively. The same volume of ASW without elevated salt level was added to the control cultures and another set of media blanks. Before addition to the cultures ASW solutions were sterilized by filtration through Filtropur S 0.2 µm filters (Sarstedt AG and Co. KG, Germany).

5.6. Extraction

Extraction of the cultures was performed as described in Vidoudez & Pohnert (2012) with modifications. Briefly, after collection of the cells from 40 mL of cultures on Whatman GF/C filters (1.2 µm pore size) (GE Healthcare, US) under vacuum (750 mbar), the endometabolome was extracted by addition of ice-cold extraction mix (1 mL methanol : ethanol : choloroform, 1:3:1, v:v:v) to the filters in 1.5 mL Eppendorf Safe-Lock tubes (Eppendorf Quality, Eppendorf AG, Germany). Cells were disrupted with ultrasonication in an ultrasonic cleaner Emmi-D280 (Emag AG, Germany) for 10 min, and cell debris was sedimented by centrifugation at 30,000g at 4 °C for 15 min. Supernatants were transferred in 1.5 mL glass vials. Volumes for GC- and LC-MS samples were normalized according to the cell amounts in the cultures. For the media blanks the average volume of the culture's samples was prepared. The samples were evaporated under vacuum. Dried samples were kept under argon and stored at -20 °C before analysis.

5.7. Sample preparation

Samples for the GC-MS analysis were prepared as described in Vidoudez & Pohnert (2012) with modifications. Briefly, dried samples contained aliquots equivalent to $5 \cdot 10^6$ cells and pooled quality control (QC) samples with equal volumes from each extract were reconstituted in 25 µL of pyridine (Chromasolv Plus, Sigma-Aldrich) containing 20 mg mL^{-1} methoxyamine monohydrochloride (Sigma-Aldrich), heated at 60 °C for 1 hour and incubated at a room temperature overnight. 20 µL of samples were transferred into vials with inserts, and to each sample 20 µL of *N,O*-bis(trimethylsilyl)trifluoroacetamide (Thermo) were added. To one QC samples 1 µL of a C7–C40 alkane standard mix, 100 µg mL^{-1} in hexane (diluted 1:10 from the 1 mg mL^{-1} standard from Sigma-Aldrich) was added. Samples were heated at 60 °C for 1 hour and directly measured.

For the LC-MS analysis aliquots equivalent to $3 \cdot 10^6$ cells and pooled quality control (QC) samples with equal volumes from each extract were reconstituted in 150 µL of a mixture of methanol : acetonitrile : water (5:9:1, v:v:v).

5.8. Standards

For GC-MS measurement, samples of standards were dried under vacuum and derivatised in the same way as experimental samples. Final concentrations of standards made up 100 µg mL^{-1}. To 40 µl of each standard sample 1 µL of a C7–C40 alkane standard mix, 100 µg mL^{-1} in hexane was added (final concentration of C7–C40 alkane standard mix was 2.44 µg mL^{-1}).

For LC-MS measurement, solutions of the standards were prepared by dissolving the standard in a mixture of methanol : acetonitrile : water (5:9:1, v:v:v) with the final concentration of 1 mg mL^{-1}. *N*γ-acetyldiaminobutyrate and cysteinolic acid were dissolved in water.

The list of measured standards is presented in the supplementary information (Appendix S1).

5.9. GC-MS measurement

GC-MS measurements were performed on a Q-Exactive Orbitrap mass spectrometer connected to a Trace 1310 Gas Chromatograph with a TriPlus RSH Autosampler (Thermo Scientific, Bremen, Germany). The gas chromatograph was equipped with a Zebron ZB-SemiVolatiles column (30 m × 0.25 mm × 0.25 µm, Phenomenex, USA). Helium was used as a carrier gas with a flow rate of 1 mL min^{-1}.

For the electron ionization (EI) mode temperature of the injector was 250 °C, transfer line 250 °C, the auxiliary zone 280 °C, and the ion source 300 °C. For the chemical ionization (CI) mode temperature of the ion source was 180 °C, methane was used as an ionization gas with a flow rate of 1.5 mL min^{-1}. The injected volume of samples was 1 µL, for EI mode split ratio varied (Table S4), CI samples were recorded in the splitless mode.

Data were recorded in full scan profile mode across a mass range from 50 to 600 *m/z* in EI mode. Full scan profile mode with a mass range from 80 to 1000 *m/z* was used for the CI mode, the ionization energy was 70 eV.

Due to the high intensity of the proline peak at the beginning of the GC chromatogram (Fig. S18), split ratios had to be high enough to not overload column and detector. However, detection of low concentrated metabolites was limited at those split ratios. To circumvent this, all samples were injected twice and measured with two different methods. The first method ("Proline method") was run at a sufficiently high split rate to detect proline without overloading the system and MS-acquisition was terminated after elution of proline (Table S4, Appendix S2). The second method ("After proline method") was run with a lower split ratio, the same temperature gradient (Appendix S3), but acquisition started after the elution of proline. For data analysis, preprocessed data for both measurements were combined, with data up to retention time of proline taken from the first measurement and data after retention time of proline taken from the second one.

5.10. LC-MS measurement

Samples for LC-MS analysis were measured with a Dionex Ultimate 3000 system coupled to a Q-Exactive Plus Orbitrap mass spectrometer (Thermo Scientific, Bremen, Germany). The measurements were performed in positive and negative modes, heated electrospray ionization was used to generate molecular ions. The duration of the method was 14.5 min with an MS runtime from 0.5 min to 9 min. Separation of the samples was performed on a SeQuant ZIC-HILIC column (5 µm, 200 Å, 150x2.1 mm, Merck, Germany), equipped with SeQuant ZIC-HILIC guard column (20x2.1 mm, Merck, Germany). Eluent A consisted of water with 2% acetonitrile and 0.1% formic acid, eluent B of 90% acetonitrile with 10% water and 1 mmol L^{-1} ammonium acetate. The flow rate was set to 0.6 mL min^{-1}, the gradient started with 85 % solvent B which was held for 4.0 min, gradient to 0 % of solvent B (4.0 – 5.0 min), hold 0 % B (5.0 – 7.0 min), gradient to 100 % of B (7.0 – 8.0 min), hold 100 % B (8.0 – 10.0 min), gradient to 85 % of B (10.0 – 10.5 min), hold 85 % B (10.5 – 12.5 min).

The instrument settings can be found in the supplementary information Appendix S4.

5.11. GC-MS data pre-processing

GC-MS data pre-processing was performed as described in Stettin et al., (2020). Briefly, raw files were converted into .mzXML format using Proteowizard Suite (proteowizard.sourceforge.net) with vendor peak picking enabled. Data were pre-processed with an R script (Stettin et al., 2020), which includes the XCMS package (Smith et al., 2006), CAMERA package (Kuhl et al., 2012), and MetaMS package (Wehrens et al., 2014). Obtained data was processed further with StatTarget package (Luan et al., 2018) for quality control based signal drift correction. All settings were used as published except minimum fragments for features grouping was set to 5 (Stettin et al., 2020).

5.12. LC-MS data pre-processing

Obtained raw data were preprocessed using Compound Discoverer version 3.1 (Thermo Fisher Scientific). The standard workflow (Untargeted Metabolomics with Statistics Detect Unknowns with ID Using Online Databases and mzLogic) with default settings was applied. Peak picking and deconvolution were performed for each algae species experiment separately.

5.13. Statistical analysis

Statistical analysis was performed for signals of which the average peak area of treated or control cultures was at least 5 times higher than in blank samples. Statistical analysis was conducted using Metaboanalyst 4.0 (Chong et al., 2018). Data was log-transformed and auto-scaled. Statistically significantly dysregulated compounds were detected using volcano plots with fold change more than 2 and false discovery rate adjusted *p*-value less than 0.05 with unequal group variance.

Comparison of dysregulated unidentified metabolites compositions between species was performed by comparing retention time and *m*/*z* values of the molecular ion for LC-MS results, and retention index, *m*/*z*, and MS-spectrum of the fragment with the highest intensity for GC-MS results.

Since for one LC-MS sample of *T. pseudonana* control culture (extracted 96 hours after the treatment) values highly differed from the rest of the samples, the sample was considered an outlier and was not included in further analysis (Fig. S19). One LC-MS control sample of *S. marinoi* (extracted 96 hours after the treatment) was lost during workup.

5.14. Venn diagrams

The Venn diagrams were made using the web application BioVenn (Hulsen et al., 2008).

5.15. Identification of metabolites

Identification of metabolites detected with GC-MS analysis was conducted using the NIST 2011 Mass Spectral Library database (National Institute of Standards and Technology, USA), MetFrag (Ruttkies et al., 2016) and MS-Finder platforms (Tsugawa et al., 2016). Results were manually checked for processing artifacts.

Since EI spectra in Orbitrap GC/MS often lack the molecular ion, we supported the identification of candidate metabolites by additional CI-measurements. The CI mass spectra were checked for the presence of molecular ions.–CH_4 neutral loss and +C_2H_5 and +C_3H_4 adducts to confirm the elemental composition.

The final verification of unknowns was done by comparison of mass spectra and retention index (accepted difference ≤ 3 units) with analytical standards.

Identification of unknowns detected with LC-MS analysis was performed using Sirius version 4.4.29 (Dührkop et al., 2019). Depending on the tree fragmentation score (Böcker and Dührkop, 2016), and the percentage of CSI:FingerID tool (Dührkop et al., 2015) putative identification of unknowns was performed.

The identity of unknowns was established by comparison of retention time and MS1 spectra with chemical standards (accepted difference ≤ 0.2 min, < 5 ppm). For betaine, pipecolinic acid, cysteinolic acid, methionine sulfoxide, *N*,*N*-dimethylarginine, ectoine, *N*γ-acetyldiaminobutyrate, acetylcarnitine, propionylcarnitine, butyrylcarnitine, and isovalerylcarnitine also MS2 spectra for both external and internal standards were recorded and compared manually.

Acknowledgements

The authors would like to thank Dr. Steffen Neumann (IPB Halle) for the help in repositing the MS-data in the MetaboLights database. We acknowledge funding by the state of Thuringia 2015 FGI0021 co-supported by the EU EFRE program and by the Deutsche Forschungsgemeinschaft (DFG, German Research Foundation) under Germany´s Excellence Strategy – EXC 2051 – Project-ID 081021-42 “Balance of the Microverse”. VN and GP thank the Gordon and Betty Moore Foundation for funding within the Symbiochip project.

Appendix A. Supplementary data

650

651 ## References

652 Adams, P., Thomas, J.C., Vernon, D.M., Bohnert, H.J., Jensen, R.G., 1992. Distinct
653 cellular and organismic responses to salt stress. Plant Cell Physiol. 33, 1215–1223.
654 https://doi.org/10.1093/oxfordjournals.pcp.a078376

655 Armbrust, E.V., Berges, J.A., Bowler, C., Green, B.R., Martinez, D., Putnam, N.H.,
656 Zhou, S., Allen, A.E., Apt, K.E., Bechner, M., Brzezinski, M.A., Chaal, B.K., Chiovitti,
657 A., Davis, A.K., Demarest, M.S., Detter, J.C., Glavina, T., Goodstein, D., Hadi, M.Z.,
658 Hellsten, U., Hildebrand, M., Jenkins, B.D., Lau, W.W.Y., Lane, T.W., Larimer, F.W.,
659 Lippmeier, J.C., Lucas, S., Montsant, A., Obornik, M., Parker, M.S., Palenik, B.,
660 Pazour, G.J., Richardson, P.M., Rynearson, T.A., Saito, M.A., Schwartz, D.C.,
661 Thamatrakoln, K., Valentin, K., Vardi, A., Wilkerson, F.P., Rokhsar, D.S., 2004. The
662 genome of the diatom *Thalassiosira pseudonana*: Ecology, evolution, and metabolism.
663 Science 306, 79–87. https://doi.org/10.1126/science.1101156

664 Bergeijk, S.A. Van, Zee, C. Van Der, Stal, L.J., 2003. Uptake and excretion of
665 dimethylsulphoniopropionate is driven by salinity changes in the marine benthic diatom
666 *Cylindrotheca closterium*. Eur. J. Phycol. 38, 341–349.
667 https://doi.org/10.1080/09670260310001612600

668 Blunden, G., Smith, B.E., Irons, M.W., Yang, M.-H., Roch, O.G., Patel, A. V, 1992.
669 Betaines and tertiary sulphonium compounds from 62 species of marine algae.
670 Biochem. Syst. Ecol. 20, 373–388. https://doi.org/10.1016/0305-1978(92)90050-N

671 Böcker, S., Dührkop, K., 2016. Fragmentation trees reloaded. J. Cheminform. 8, 1–26.
672 https://doi.org/10.1186/s13321-016-0116-8

673 Bowler, C., Allen, A.E., Badger, J.H., Grimwood, J., Jabbari, K., Kuo, A., Maheswari,
674 U., Martens, C., Maumus, F., Otillar, R.P., Rayko, E., Salamov, A., Vandepoele, K.,
675 Beszteri, B., Gruber, A., Heijde, M., Katinka, M., Mock, T., Berges, J.A., Brownlee,
676 C., Cadoret, J., Chiovitti, A., Valentin, K., Choi, C.J., Coesel, S., Martino, A. De,
677 Detter, J.C., Durkin, C., Falciatore, A., Lopez, P.J., Lucas, S., Lindquist, E., Lommer,
678 M., Napoli, C., Obornik, M., Parker, M.S., Petit, J., Porcel, B.M., 2008. The
679 *Phaeodactylum* genome reveals the evolutionary history of diatom genomes. Nature
680 456, 239–244. https://doi.org/10.1038/nature07410

681 Branda, L.E., 1984. The salinity tolerance of forty-six marine phytoplankton isolates.
682 Estuar. Coast. Shelf Sci. 18, 543–556. https://doi.org/10.1016/0272-7714(84)90089-1

683 Chong, J., Soufan, O., Li, C., Caraus, I., Li, S., Bourque, G., Wishart, D.S., Xia, J.,
684 2018. MetaboAnalyst 4.0: Towards more transparent and integrative metabolomics
685 analysis. Nucleic Acids Res. 46, 486–494. https://doi.org/10.1093/nar/gky310

686 Czech, L., Hermann, L., Stöveken, N., Richter, A.A., Id, A.H., Smits, S.H.J., Heider,
687 J., Bremer, E., 2018. Role of the extremolytes ectoine and hydroxyectoine as stress
688 protectants and nutrients: Genetics, phylogenomics, biochemistry, and structural
689 analysis. Genes (Basel). 9, 1–58. https://doi.org/10.3390/genes9040177

690 Dawson, H.M., Heal, K.R., Boysen, A.K., Carlson, L.T., Ingalls, A.E., Young, J.N.,
691 2020. Potential of temperature- and salinity-driven shifts in diatom compatible solute
692 concentrations to impact biogeochemical cycling within sea ice. Elem. Sci. Anthr. 8,
693 25. https://doi.org/10.1525/elementa.421

694 Dickson, D.M., Kirst, G.O., 1987. Osmotic adjustment in marine eukaryotic algae: The
695 role of inorganic ions, quaternary ammonium, tertiary sulphonium and carbohydrate
696 solutes. New Phytol. 106, 645–655. https://doi.org/10.1111/j.1469-
697 8137.1987.tb00165.x

698 Downing, A.B., Wallace, G.T., Yancey, P.H., 2018. Organic osmolytes of amphipods
699 from littoral to hadal zones: Increases with depth in trimethylamine N-oxide , scyllo-
700 inositol and other potential pressure counteractants. Deep. Res. Part I 138, 1–10.
701 https://doi.org/10.1016/j.dsr.2018.05.008

702 Durack, P.J., Wijffels, S.E., 2010. Fifty-year trends in global ocean salinities and their
703 relationship to broad-scale warming. J. Clim. 23, 4342–4362.
704 https://doi.org/10.1175/2010JCLI3377.1

705 Dührkop, K., Fleischauer, M., Ludwig, M., Aksenov, A.A., Melnik, A. V, Meusel, M.,
706 Dorrestein, P.C., Rousu, J., Böcker, S., 2019. SIRIUS 4: A rapid tool for turning tandem
707 mass spectra into metabolite structure information. Nat. Methods 16, 299–302.
708 https://doi.org/10.1038/s41592-019-0344-8

709 Dührkop, K., Shen, H., Meusel, M., Rousu, J., Böcker, S., 2015. Searching molecular
710 structure databases with tandem mass spectra using CSI:FingerID. Proc. Natl. Acad.
711 Sci. 112, 12580–12585. https://doi.org/10.1073/pnas.1509788112

712 Fenizia, S., Thume, K., Wirgenings, M., Pohnert, G., 2020. Ectoine from bacterial and
713 algal origin is a compatible solute in microalgae. Mar. Drugs 18, 1–13.
714 https://doi.org/10.3390/md18010042

715 Field, C.B., Behrenfeld, M.J., Randerson, J.T., Falkowski, P., 1998. Primary production
716 of the biosphere: Integrating terrestrial and oceanic components. Science. 281, 237–
717 240. https://doi.org/10.1126/science.281.5374.237

718 Fukutoku, Y., Yamada, Y., 1981. Sources of proline-nitrogen in water-stressed soybean
719 (*Glycine max* L.) I. protein metabolism and proline accumulation. Plant Cell Physiol.
720 22, 1397–1404. https://doi.org/10.1093/oxfordjournals.pcp.a076292

721 García, N., López-elías, J.A., Miranda, A., Martínez-Porchas, M., Huerta, N., García,
722 A., 2012. Effect of salinity on growth and chemical composition of the diatom
723 *Thalassiosira weissflogii* at three culture phases. Lat. Am. J. Aquat. Res. 40, 435–440.
724 https://doi.org/10.3856/vol40-issue2-fulltext-18

725 Gebser, B., Pohnert, G., 2013. Synchronized regulation of different zwitterionic
726 metabolites in the osmoadaption of phytoplankton. Mar. Drugs 11, 2168–2182.
727 https://doi.org/10.3390/md11062168

728 Gilmour, D.J., Hipkins, M.F., Boney, A.D., 1982. The effect of salt stress on the
729 primary processes of photosynthesis in *Dunaliella tertiolecta*. Plant Sci. Lett. 26, 325–
730 330. https://doi.org/10.1016/0304-4211(82)90107-9

731 Gilmour, D.J., Hipkins, M.F., Webber, A.N., Baker, N.R., Boney, A.D., 1985. The
732 effect of ionic stress on photosynthesis in *Dunaliella tertiolecta*. Chlorophyll
733 fluorescence kinetics and spectral characteristics. Planta 163, 250–256.
734 https://doi.org/10.1007/BF00393515

735 Glaser, K., Karsten, U., 2020. Salinity tolerance in biogeographically different strains
736 of the marine benthic diatom *Cylindrotheca closterium* (Bacillariophyceae). J. Appl.
737 Phycol. 32, 3809–3816. https://doi.org/10.1007/s10811-020-02238-6

738 Hellebust, J.A., 1976. Osmoregulation. Annu. Rev. Plant Physiol. 27, 485–505.
739 https://doi.org/10.1146/annurev.pp.27.060176.002413

740 Hulsen, T., Vlieg, J. De, Alkema, W., 2008. BioVenn – a web application for the
741 comparison and visualization of biological lists using area-proportional Venn diagrams.
742 BMC Genomics 9, 1–6. https://doi.org/10.1186/1471-2164-9-488

743 Jaramillo-Madrid, A.C., Ashworth, J., Ralph, P.J., 2020. Levels of diatom minor sterols
744 respond to changes in temperature and salinity. J. Mar. Sci. Eng. 8, 1–14.
745 https://doi.org/10.3390/jmse8020085

Johansson, O.N., Töpel, M., Pinder, M.I.M., Kourtchenko, O., Blomberg, A., Godhe, A., Clarke, A.K., 2019. *Skeletonema marinoi* as a new genetic model for marine chain-forming diatoms. Nat. Sci. Reports 9, 1–10. https://doi.org/10.1038/s41598-019-41085-5

Joshi, V., Fei, Z., Joung, J., Jander, G., 2010. Interdependence of threonine, methionine and isoleucine metabolism in plants accumulation and transcriptional regulation under abiotic stress. Amino Acids 39, 933–947. https://doi.org/10.1007/s00726-010-0505-7

Kanehisa, M., Goto, S., 2000. KEGG : Kyoto Encyclopedia of Genes and Genomes. Nucleic Acids Res. 28, 27–30. https://doi.org/10.1093/nar/28.1.27

Keller, M.D., Kiene, R.P., Matrai, P.A., Bellows, W.K., 1999. Production of glycine betaine and dimethylsulfoniopropionate in marine phytoplankton. I. Batch cultures. Mar. Biol. 135, 237–248. https://doi.org/10.1007/s002270050621

Kets, E.P.W., Bont, J.A.M. De, 1997. Effect of carnitines on *Lactobacillus plantarum* subjected to osmotic stress. FEMS Microbiol. Lett. 146, 205–209. https://doi.org/10.1111/j.1574-6968.1997.tb10194.x

Kim, K.H., Jia, B., Jeon, C.O., 2017. Identification of trans-4-hydroxy-l-proline as a compatible solute and its biosynthesis and molecular characterization in *Halobacillus halophilus*. Front. Microbiol. 8, 1–11. https://doi.org/10.3389/fmicb.2017.02054

Kirst, G.O., 1989. Salinity tolerance of eukaryotic marine algae. Annu. Rev. Plant Physiol. Plant Mol. Biol. 40, 21–53. https://doi.org/10.1146/annurev.pp.41.060190.000321

Kissoudis, C., Kalloniati, C., Flemetakis, E., Madesis, P., Labrou, N.E., Tsaftaris, A., Nianiou-Obeidat, I., 2015. Stress-inducible GmGSTU4 shapes transgenic tobacco plants metabolome towards increased salinity tolerance. Acta Physiol. Plant. 37, 102. https://doi.org/10.1007/s11738-015-1852-5

Klages, K., Boldings, H., Smith, G.S., 1999. Accumulation of myo-inositol in *Actinidia* seedlings subjected to salt stress. Ann. Bot. 84, 521–527. https://doi.org/10.1006/anbo.1999.0946

Kuhl, C., Tautenhahn, R., Bo, C., Larson, T.R., Neumann, S., 2012. CAMERA: An integrated strategy for compound spectra extraction and annotation of liquid chromatography/mass spectrometry data sets. Anal. Chem. 84, 283–289. https://doi.org/10.1021/ac202450g

778 Landa, M., Burns, A.S., Roth, S.J., Moran, M.A., 2017. Bacterial transcriptome
779 remodeling during sequential co-culture with a marine dinoflagellate and diatom. ISME
780 J. 11, 2677–2690. https://doi.org/10.1038/ismej.2017.117

781 Laws, E.A., 2013. Evaluation of *in situ* phytoplankton growth rates: A synthesis of data
782 from varied approaches. Ann. Rev. Mar. Sci. 5, 247–268.
783 https://doi.org/10.1146/annurev-marine-121211-172258

784 Leimer, K.R., Rice, R.H., Gehrke, C.W., 1977. Complete mass spectra of the per-
785 trimethylsilylated amino acids. J. Chromatogr. A 141, 355–375.
786 https://doi.org/10.1016/S0021-9673(00)93539-8

787 Liu, M.S., Hellebust, J.A., 1976. Regulation of proline metabolism in the marine centric
788 diatom *Cyclotella cryptica*. Can. J. Bot. 54, 949–959. https://doi.org/10.1139/b76-099

789 Luan, H., Ji, F., Chen, Y., Cai, Z., 2018. statTarget: A streamlined tool for signal drift
790 correction and interpretations of quantitative mass spectrometry-based omics data.
791 Anal. Chim. Acta 1036, 66–72. https://doi.org/10.1016/j.aca.2018.08.002

792 Maier, I., Calenberg, M., 1994. Effect of extracellular Ca^{2+} and Ca^{2+}-antagonists on the
793 movement and chemoorientation of male gametes of *Ectocarpus siliculosus*
794 (Phaeophyceae). Bot. Acta 107, 451–460. https://doi.org/10.1111/j.1438-
795 8677.1994.tb00820.x

796 Martino, A. De, Meichenin, A., Shi, J., Pan, K., Bowler, C., 2007. Genetic and
797 phenotypic characterization of *Phaeodactylum tricornutum* (Bacillariophyceae)
798 accessions. J. Phycol. 43, 992–1009. https://doi.org/10.1111/j.1529-
799 8817.2007.00384.x

800 Medlin, L.K., Kaczmarska, I., 2004. Evolution of the diatoms: V. Morphological and
801 cytological support for the major clades and a taxonomic revision. Phycologia 43, 245–
802 270. https://doi.org/10.2216/i0031-8884-43-3-245.1

803 Mentzen, W.I., Peng, J., Ransom, N., Nikolau, B.J., Wurtele, E.S., 2008. Articulation
804 of three core metabolic processes in Arabidopsis: Fatty acid biosynthesis, leucine
805 catabolism and starch metabolism. BMC Plant Biol. 8, 1–15.
806 https://doi.org/10.1186/1471-2229-8-76

807 Mimura, H., Nagata, S., Matsumoto, T., 1994. Concentrations and compositions of
808 internal free amino acids in a halotolerant *Brevibacterium sp*. in response to salt stress.
809 Biosci. Biotechnol. Biochem. 58, 1873–1874. https://doi.org/10.1271/bbb.58.1873

Moulin, M., Deleu, C., Larher, F., 2000. L-Lysine catabolism is osmo-regulated at the level of lysine-ketoglutarate reductase and saccharopine dehydrogenase in rapeseed leaf discs. Plant Physiol. Biochem. 38, 577–585. https://doi.org/10.1016/S0981-9428(00)00777-4

Neshich, I.A.P., Kiyota, E., Arruda, P., 2013. Genome-wide analysis of lysine catabolism in bacteria reveals new connections with osmotic stress resistance. ISME J. 7, 2400–2410. https://doi.org/10.1038/ismej.2013.123

Ochsenkühn, M.A., Röthig, T., D'Angelo, C., Wiedenmann, J., Voolstra, C.R., 2017. The role of floridoside in osmoadaptation of coral-associated algal endosymbionts to high-salinity conditions. Sci. Adv. 3, e1602047. https://doi.org/10.1126/sciadv.1602047

Peters, P., Galinski, E.A., Trüper, H.G., 1990. The biosynthesis of ectoine. FEMS Microbiol. Lett. 71, 157–162. https://doi.org/10.1111/j.1574-6968.1990.tb03815.x

Rijstenbil, J.W., 2003. Effects of UVB radiation and salt stress on growth, pigments and antioxidative defence of the marine diatom *Cylindrotheca closterium*. Mar. Ecol. Prog. Ser. 254, 37–47.

Ruttkies, C., Schymanski, E.L., Wolf, S., Hollender, J., Neumann, S., 2016. MetFrag relaunched: incorporating strategies beyond *in silico* fragmentation. J. Cheminform. 8, 1–16. https://doi.org/10.1186/s13321-016-0115-9

Scholz, B., Liebezeit, G., 2012. Compatible solutes in three marine intertidal microphytobenthic Wadden Sea diatoms exposed to different salinities. Eur. J. Phycol. 47, 393–407. https://doi.org/10.1080/09670262.2012.720714

Smith, C.A., Want, E.J., O'Maille, G., Abagyan, R., Siuzdak, G., 2006. XCMS: Processing mass spectrometry data for metabolite profiling using nonlinear peak alignment, matching, and identification. Anal. Chem. 78, 779–787. https://doi.org/10.1021/ac051437y

Stettin, D., Poulin, R.X., Pohnert, G., 2020. Metabolomics benefits from GC Orbitrap – comparison of low- and high-resolution GC-MS. Metabolites 10, 143. https://doi.org/10.3390/metabo10040143

Sugie, K., Fujiwara, A., Nishino, S., Kameyama, S., Harada, N., 2020. Impacts of temperature, CO_2, and salinity on phytoplankton community composition in the western Arctic Ocean. Front. Mar. Sci. 6, 821. https://doi.org/10.3389/fmars.2019.00821

Thomas, M.K., Kremer, C.T., Klausmeier, C.A., Litchman, E., 2012. A global pattern of thermal adaptation in marine phytoplankton. Science. 338, 1085–1088. https://doi.org/10.1126/science.1224836

Thume, K., Gebser, B., Chen, L., Meyer, N., Kieber, D.J., Pohnert, G., 2018. The metabolite dimethylsulfoxonium propionate extends the marine organosulfur cycle. Nature 563, 412–415. https://doi.org/10.1038/s41586-018-0675-0

Trinchant, J., Boscari, A., Spennato, G., Sype, G. Van De, Rudulier, D. Le, 2004. Proline betaine accumulation and metabolism in alfalfa plants under sodium chloride stress. Exploring its compartmentalization in nodules. Plant Physiol. 135, 1583–1594. https://doi.org/10.1104/pp.103.037556.1

Tsugawa, H., Kind, T., Nakabayashi, R., Yukihira, D., Tanaka, W., Cajka, T., Saito, K., Fiehn, O., Arita, M., 2016. Hydrogen rearrangement rules: computational ms/ms fragmentation and structure elucidation using MS-FINDER software. Anal. Chem. 88, 7946–7958. https://doi.org/10.1021/acs.analchem.6b00770

Vidal, T., Calado, A.J., Moita, M.T., Cunha, M.R., 2017. Phytoplankton dynamics in relation to seasonal variability and upwelling and relaxation patterns at the mouth of Ria de Aveiro (West Iberian Margin) over a four-year period. PLoS One 12, 1–25. https://doi.org/10.1371/journal.pone.0177237

Vidoudez, C., Pohnert, G., 2012. Comparative metabolomics of the diatom *Skeletonema marinoi* in different growth phases. Metabolomics 8, 654–669. https://doi.org/10.1007/s11306-011-0356-6

Wehrens, R., Weingart, G., Mattivi, F., 2014. metaMS : An open-source pipeline for GC – MS-based untargeted metabolomics. J. Chromatogr. B 966, 109–116. https://doi.org/10.1016/j.jchromb.2014.02.051

Weinisch, L., Ku, S., Roth, R., Grimm, M., Roth, T., Daili, J., Netz, A., Pierik, A.J., Filker, S., 2018. Identification of osmoadaptive strategies in the halophile, heterotrophic ciliate *Schmidingerothrix salinarum*. PloS Biol. 16, 1–29. https://doi.org/10.1371/journal.pbio.2003892

Yamamoto, M., Chiba, T., Tuji, A., 2017. Salinity responses of benthic diatoms inhabiting tidal flats. Diatom Res. 32, 243–250. https://doi.org/10.1080/0269249X.2017.1366951

874 Yancey, P.H., 2005. Organic osmolytes as compatible, metabolic and counteracting
875 cytoprotectants in high osmolarity and other stresses. J. Exp. Biol. 208, 2819–2830.
876 https://doi.org/10.1242/jeb.01730

877 Zhang, J., Chen, G., Zhao, P., Zhou, Q., Zhao, X., 2017. The abundance of certain
878 metabolites responds to drought stress in the highly drought tolerant plant *Caragana*
879 *korshinskii*. Acta Physiol. Plant. 39, 116. https://doi.org/10.1007/s11738-017-2412-y

880 Zhang, J., Yang, D., Li, M., Shi, L., 2016. Metabolic profiles reveal changes in wild
881 and cultivated soybean seedling leaves under salt stress. PLoS One 11, 1–17.
882 https://doi.org/10.1371/journal.pone.0159622

883 Zika, J.D., Skliris, N., Blaker, A.T., Marsh, R., Nurser, A.J.G., Josey, S.A., 2018.
884 Improved estimates of water cycle change from ocean salinity: The key role of ocean
885 warming. Environ. Res. Lett. 13, 074036. https://doi.org/10.1088/1748-9326/aace42

886

887

Figures and Tables

Figure 1: Pairwise PCA plots for *T. pseudonana* endometabolome samples extracted 24 (A, B) and 96 (C, D) hours after salinity increase. PCA plots of all data analyzed together (E, F). Panels A, C, and E show results from GC-MS. Panels B, D, and F result from the analysis of LC-MS data; the number of replicates analyzed is 4 – 5 (see Experimental 5.13.).

Figure 2: Pairwise PCA plots for *P. tricornutum* endometabolome samples extracted 24 (A, B) and 96 (C, D) hours after the salinity stress treatment. PCA plots of all data analyzed together (E, F). Panels A, C, and E show results from GC-MS. Panels B, D, and F result from the analysis of LC-MS data; the number of replicates analyzed is 5.

Figure 3: Pairwise PCA plots for *S. marinoi* endometabolome samples extracted 24 (A, B) and 96 (C, D) hours after the salinity stress treatment. PCA plots of all data analyzed together (E, F). Panels A, C, and E show results from GC-MS. Panels B, D, and F result from the analysis of LC-MS data; the number of replicates analyzed is 4 – 5 (see Experimental 5.13.).

Figure 4: Venn diagrams for significantly dysregulated compounds of all identification levels for *P. tricornutum* (blue), *T. pseudonana* (green), and *S. marinoi* (yellow) detected with GC-MS at 24 h (A) and 96 h (B) after the salinity stress. The percentage of the total number of compounds detected for all three algae is given and numbers in brackets indicate the amount of compounds.

Figure 5: Venn diagrams for significantly dysregulated compounds of all identification levels for *P. tricornutum* (blue), *T. pseudonana* (green), and *S. marinoi* (yellow) detected with LC-MS at 24 h (A) and 96 h (B) after the salinity stress. The percentage of the total number of compounds detected for all three algae is given and numbers in brackets indicate the amount of compounds.

Table 1: Statistically significantly up-regulated metabolites in response to salinity stress. Compounds were detected with GC-MS and/or LC-MS. Only compounds are listed that were confirmed with analytical standards. Significance criteria were p-value < 0.05 and fold change > 2.

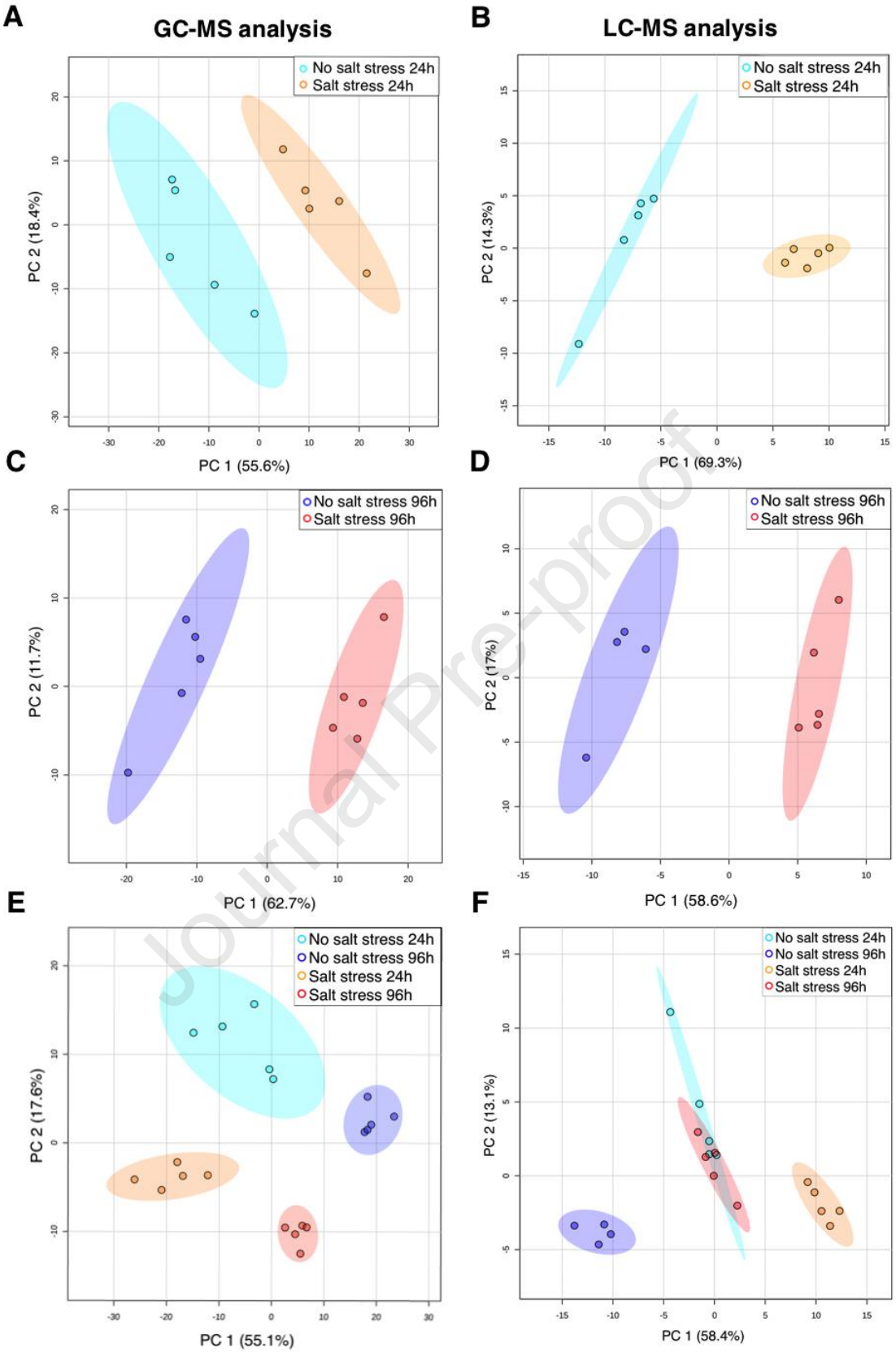
A
GC-MS analysis
No salt stress 24h
Salt stress 24h
PC 2 (18.4%)
PC 1 (55.6%)
B
LC-MS analysis
No salt stress 24h
Salt stress 24h
PC 2 (14.3%)
PC 1 (69.3%)
C
No salt stress 96h
Salt stress 96h
PC 2 (11.7%)
PC 1 (62.7%)
D
No salt stress 96h
Salt stress 96h
PC 2 (17%)
PC 1 (58.6%)
E
No salt stress 24h
No salt stress 96h
Salt stress 24h
Salt stress 96h
PC 2 (17.6%)
PC 1 (55.1%)
F
No salt stress 24h
No salt stress 96h
Salt stress 24h
Salt stress 96h
PC 2 (13.1%)
PC 1 (58.4%)

Figure 1

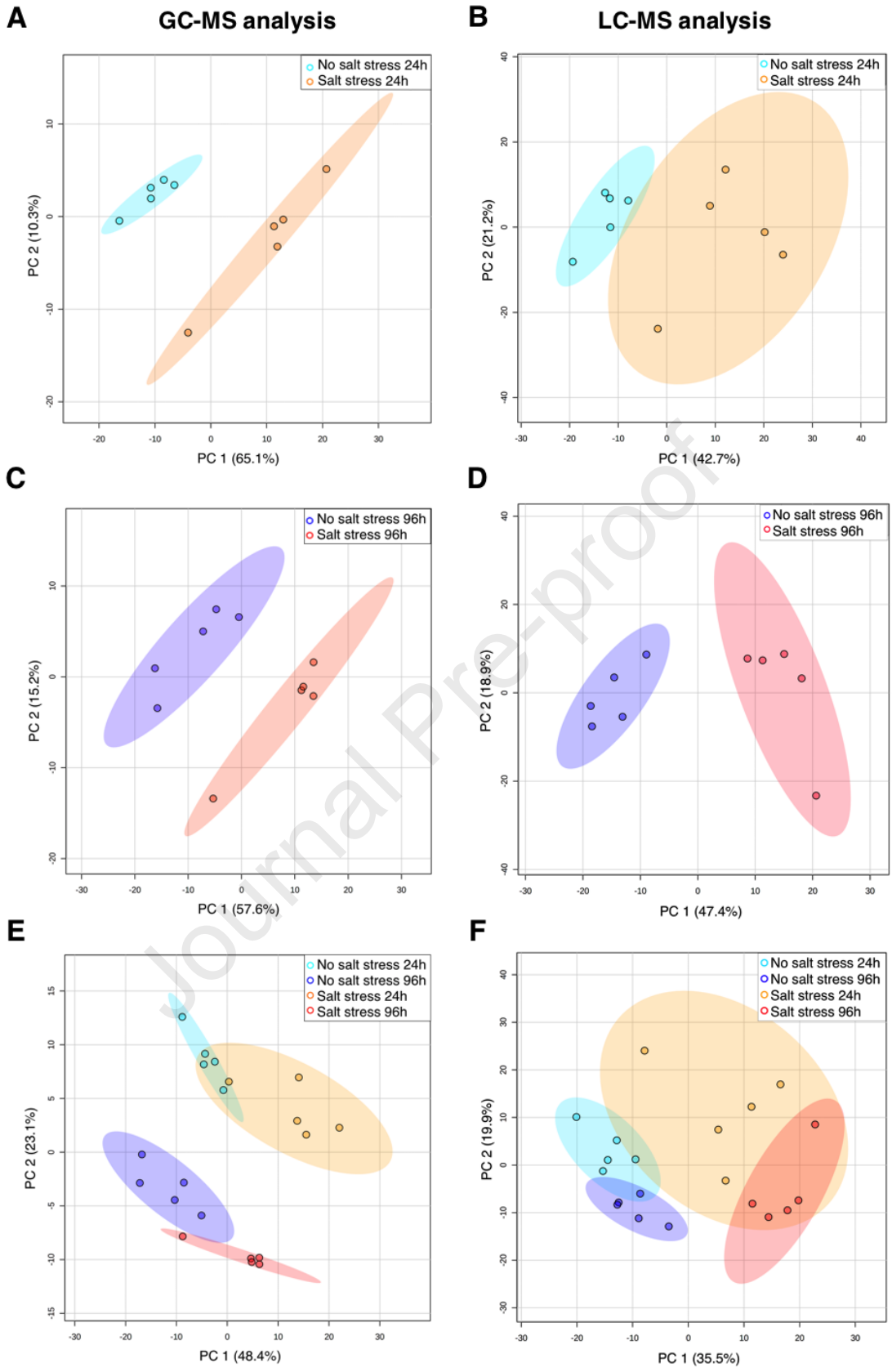
A
GC-MS analysis
No salt stress 24h
Salt stress 24h
PC 2 (10.3%)
PC 1 (65.1%)
B
LC-MS analysis
No salt stress 24h
Salt stress 24h
PC 2 (21.2%)
PC 1 (42.7%)
C
No salt stress 96h
Salt stress 96h
PC 2 (15.2%)
PC 1 (57.6%)
D
No salt stress 96h
Salt stress 96h
PC 2 (18.9%)
PC 1 (47.4%)
E
No salt stress 24h
No salt stress 96h
Salt stress 24h
Salt stress 96h
PC 2 (23.1%)
PC 1 (48.4%)
F
No salt stress 24h
No salt stress 96h
Salt stress 24h
Salt stress 96h
PC 2 (19.9%)
PC 1 (35.5%)

Figure 2

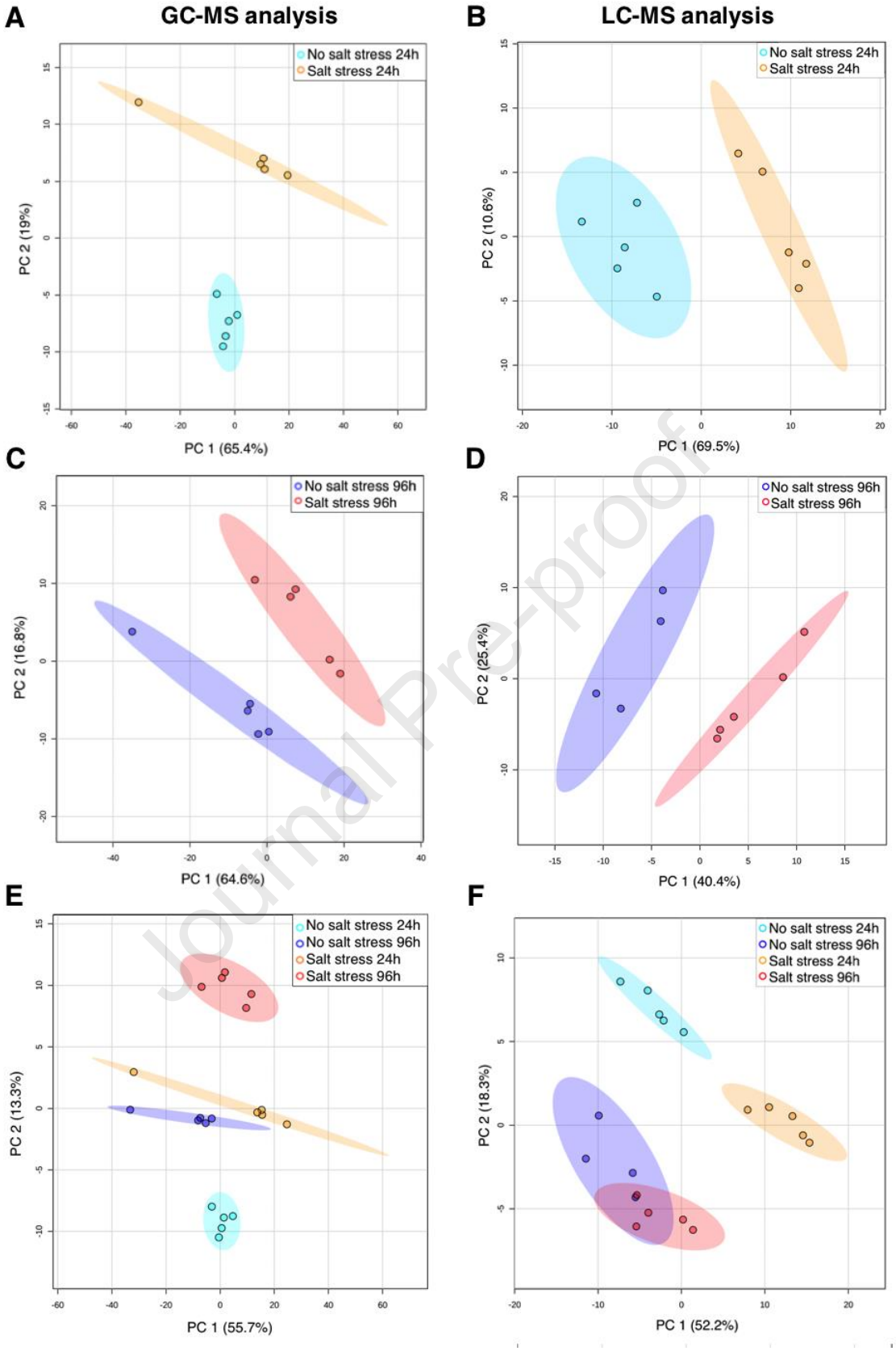

Figure 3

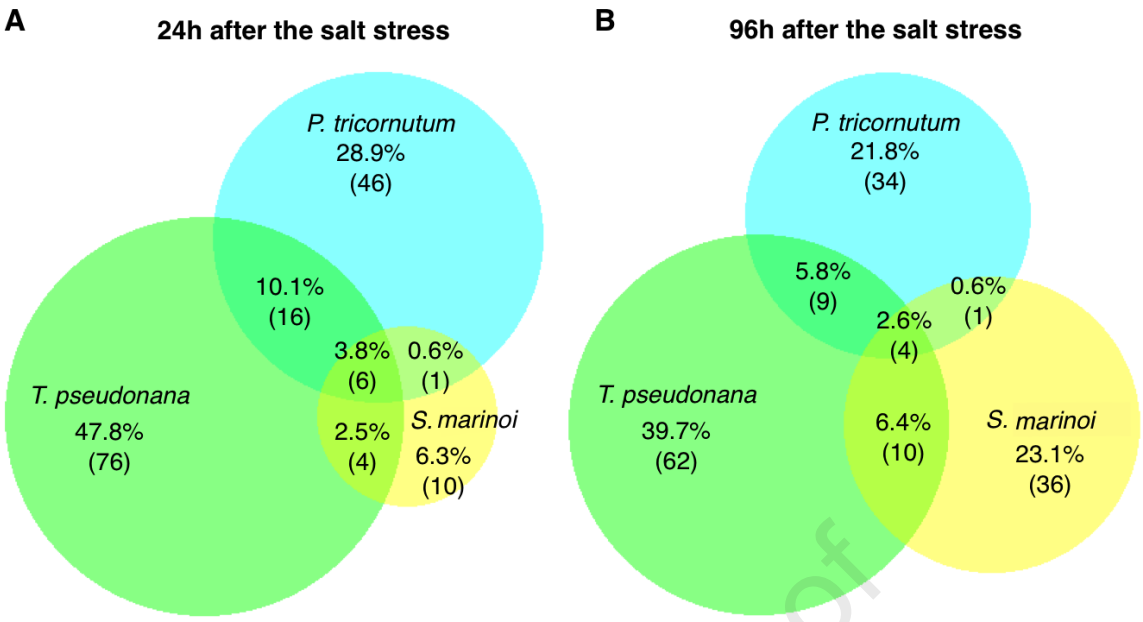

924

925 **Figure 4**

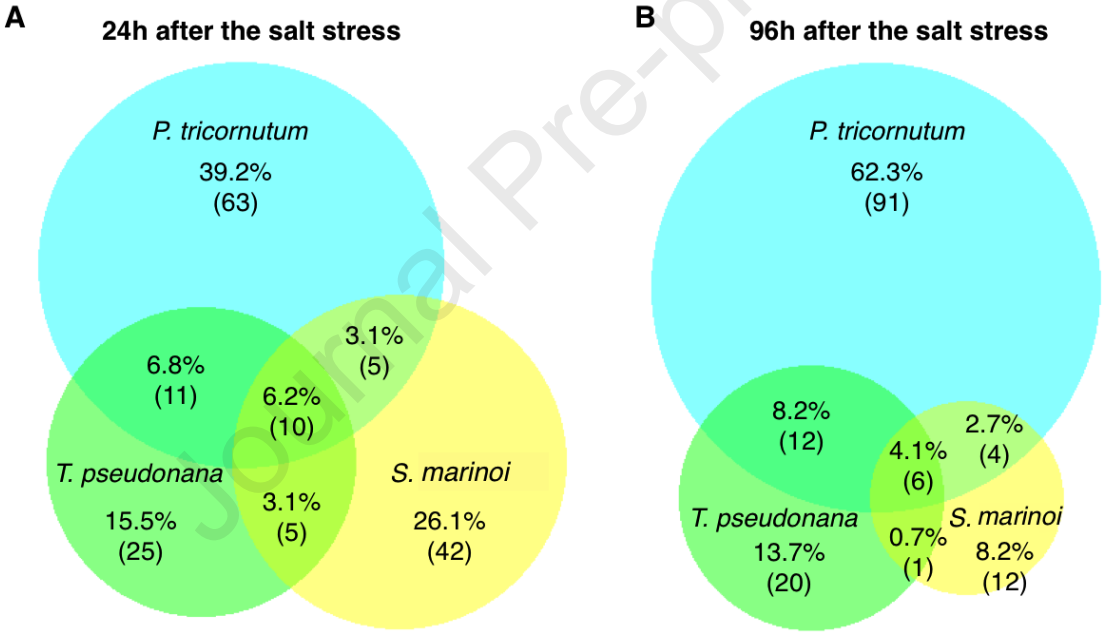

926

927 **Figure 5**

928

929 **Table 1**

Metabolite	Algae
Tyrosine	*T. pseudonana*, *P. tricornutum*, *S. marinoi*
Threonine	*T. pseudonana*, *P. tricornutum*, *S. marinoi*
Pyrrole−2−carboxylic acid	*T. pseudonana*, *P. tricornutum*, *S. marinoi*
Proline	*T. pseudonana*, *P. tricornutum*, *S. marinoi*
Pipecolate	*T. pseudonana*, *P. tricornutum*, *S. marinoi*
Phenylalanine	*T. pseudonana*, *P. tricornutum*, *S. marinoi*
Myo−Inositol	*T. pseudonana*, *P. tricornutum*, *S. marinoi*
Glyceryl−glycoside, putative	*T. pseudonana*, *P. tricornutum*, *S. marinoi*

Metabolite	Algae
4−Hydroxyproline	*T. pseudonana*, *P. tricornutum*, *S. marinoi*
Ectoine	*T. pseudonana*, *P. tricornutum*, *S. marinoi* *
Tryptophan	*T. pseudonana*, *P. tricornutum*
Threonic acid	*T. pseudonana*, *P. tricornutum*
Methionine	*T. pseudonana*, *P. tricornutum*
Mannose	*T. pseudonana*, *P. tricornutum*
Lysine	*T. pseudonana*, *P. tricornutum*
Isoleucine	*T. pseudonana*, *P. tricornutum*
Glucose	*T. pseudonana*, *P. tricornutum*
Cellobiose	*T. pseudonana*, *P. tricornutum*
Nγ-acetyldiaminobutyrate	*T. pseudonana*, *P. tricornutum*
Scyllo−Inositol	*T. pseudonana*, *S. marinoi*
Homoserine	*T. pseudonana*, *S. marinoi*
Betaine	*T. pseudonana*, *S. marinoi*
Valine	*P. tricornutum*, *S. marinoi*
Propionylcarnitine	*P. tricornutum*, *S. marinoi*
Butyrylcarnitine	*P. tricornutum*, *S. marinoi*
Cysteinolic acid	*P. tricornutum*, *S. marinoi*
Stachydrine	*T. pseudonana*
Sorbose	*T. pseudonana*
Serine	*T. pseudonana*
Pentadecanoic acid, methyl ester	*T. pseudonana*
Ornithine**	*T. pseudonana*
N-Acetyl glucosamine	*T. pseudonana*
Fructose	*T. pseudonana*
Erythrose	*T. pseudonana*
Asparagine	*T. pseudonana*
Arginine	*T. pseudonana*
Allose	*T. pseudonana*
5-oxo-Proline	*T. pseudonana*
Xylose	*P. tricornutum*
Sedoheptulose	*P. tricornutum*
Ribose	*P. tricornutum*
Putrescine	*P. tricornutum*
Methyl palmitate	*P. tricornutum*
Arginine methyl ester	*P. tricornutum*
Adenosine	*P. tricornutum*
Acetylcarnitine	*S. marinoi*
N,N-dimethylarginine	*S. marinoi*
Leucine	*S. marinoi*
Isovalerylcarnitine	*S. marinoi*
Glutamine	*S. marinoi*

930 *For *S. marinoi* ectoine was detected by evaluation of the ion trace

931 **Derivatisation of arginine results in its conversion to ornithine, and these two metabolites cannot be

932 distinguished with the GC-MS method (Leimer et al., 1977)

933

Highlights

HR LC-MS and HR GC-MS metabolomics provides insight into algal stress responses

The microalgae react to salinity stress with common adaptations in the metabolome

Individual metabolomic responses of the investigated species are observed as well

Several metabolites previously not connected to osmotic stress are identified

Algal adaptation to salinity changes occurs in a complex up-regulation of metabolites

The authors declare that are no conflicts of interest.